

# BeppoSAX observations of GRO J1744–28

R. Doroshenko<sup>1</sup>, A. Santangelo<sup>1</sup>, V. Doroshenko<sup>1</sup>, V. Suleimanov<sup>1,2</sup>, S. Piraino<sup>1,3</sup>

<sup>1</sup>*Institut für Astronomie und Astrophysik, Kepler Center for Astro and Particle Physics, Sand 1, 72076 Tübingen, Germany*

<sup>2</sup>*Kazan (Volga region) Federal University, Kremlevskaya str. 18, 42008 Kazan, Russia*

<sup>3</sup>*INAF – IASF di Palermo, via Ugo La Malfa 153, 90146 Palermo, Italy*

13 July 2021

## ABSTRACT

We present an analysis of *BeppoSAX* observations of the unique transient bursting X-ray pulsar GRO J1744–28. The observations took place in March 1997 during the decay phase of the outburst. We find that the persistent broadband X-ray continuum of the source is consistent with a cutoff power law typical for the accreting pulsars. We also detect the fluorescence iron line at 6.7 keV and an absorption feature at  $\sim 4.5$  keV, which we interpret as a cyclotron line. The corresponding magnetic field strength in the line forming region is  $\sim 3.7 \times 10^{11}$  G. Neither line is detected in the spectra of the bursts. However, additional soft thermal component with  $kT \sim 2$  keV was required to describe the burst spectrum. We briefly discuss the nature of this component and argue that among other possibilities it might be connected with thermonuclear flashes at the neutron star surface which accompany the accretion-powered bursts in the source.

**Key words:** pulsars: individual: stars: neutron stars: binaries

## 1 INTRODUCTION

The peculiar transient X-ray source GRO J1744–28 also known as the bursting pulsar, was discovered on December 2, 1995, with the Burst and Transient Source Experiment (*BATSE*), on board the Compton Gamma Ray Observatory (*CGRO*) (Fishman et al. 1995; Kouveliotou et al. 1996). Three major outbursts have been observed since the discovery. The first lasted from the end of 1995 until the beginning of 1996, the second from December 1996 until April 1997, and the third from January to May 2014 (Degenaar et al. 2014; Younes et al. 2015; D’Ài et al. 2015). The peak outburst luminosity in X-rays reaches  $L_X \sim 10^{37} - 10^{38}$  erg s<sup>-1</sup> (Woods et al. 1999), while the quiescent luminosity is  $\sim L_X \sim 10^{33}$  erg s<sup>-1</sup> (Wijnands & Wang 2002; Daigne et al. 2002; Degenaar et al. 2012). The source exhibits coherent pulsations with a period of  $\sim 0.467$  s, associated with the rotation of the neutron star i.e. is an accreting X-ray pulsar in a binary system. Finger et al. (1996) determined the orbital period and semimajor axis to be  $P_{\text{orb}} = 11.8$  days and  $a = 1.12 R_{\odot}$  ( $\sim 7.8 \times 10^{10}$  cm) respectively. The mass function was estimated to be  $f(M) = 1.36 \times 10^{-4} M_{\odot}$  implying, for the canonical neutron star mass of  $M_{\text{NS}} = 1.4 M_{\odot}$ , accretion via Roche lobe overflow from a strongly evolved red giant remnant with mass about  $0.2 - 0.7 M_{\odot}$  (Daumerie et al. 1996; Miller 1996; Sturmer & Dermer 1996; Bildsten & Brown 1997; Rappaport & Joss 1997). The photoelectric absorption does not change significantly during the outbursts and is comparable with interstellar absorption  $N_{\text{H}} \sim (5 - 6) \times 10^{22}$  cm<sup>-2</sup> in the direction of the Galactic center where the source is thought to be located at distance of  $\sim 8$  kpc (Dotani et al. 1996; Nishiuchi et al. 1999).

Probably the most unusual property of GRO J1744–28 is

the relatively short  $\sim 10$  s bursts observed from the source. Since the discovery, several thousands of bursts have been detected, all at high luminosity (Nishiuchi et al. 1999). During the bursts the flux increases by an order of magnitude, and it is often followed by a drop to below the pre-burst level for several tens of seconds to minutes depending on the burst fluence (Lewin et al. 1996; Nishiuchi et al. 1999; Younes et al. 2015). Pulsations are observed during the bursts, although with a phase shift of  $\sim 5\%$  with respect to the persistent emission (Kouveliotou et al. 1996; Strickman et al. 1996).

A similar bursting activity has been observed only in another source the transient LMXB MXB 1730–335, usually referred to as the Rapid Burster (RB) (Lewin et al. 1976; Lewin et al. 1993). For both sources, it has been suggested that the origin of the bursts could be due to accretion flow instabilities which intermittently enhance the accretion rate onto the neutron star (so-called Type II bursts). However details are still unclear. For instance, unlike the RB, Type I bursts, associated with thermonuclear flashes on the surface of neutron star, are generally thought not to occur in GRO J1744–28. On the other hand, contrary to the RB case, the duration of the GRO J1744–28 bursts is remarkably stable ( $\sim 10$  s), and a large fraction of the bursts exhibit a temporal profile characterized by a fast rise followed by an exponential decay typical of classical bursters. Type II bursts in RB have rather irregular profiles. These differences are likely related to the different magnetic field strengths of the neutron star companion, which is expected, given the presence of pulsations, to be stronger in GRO J1744–28. In the case of GRO J1744–28, Finger et al. (1996) reported an upper limit on the magnetic field strength of  $B \leq 6 \times 10^{11}$  G. This estimate is based on the requirement that the plasma at the inner edge of the ac-

cretion disk (disrupted by the magnetosphere) moves faster than the magnetic field lines as otherwise the accretion would be centrifugally inhibited (so-called “propeller” regime, Illarionov & Sunyaev 1975). Later Cui (1997) found a possible transition to the “propeller” regime in *RXTE* data at lower luminosity, which allowed for an estimate of the the magnetic field at  $\sim 2.4 \times 10^{11}$  G. Recently D’Ai et al. (2015) reported the observation of an absorption feature at  $E \sim 4.7$  keV, during the 2014 outburst of the source. Interpreting the line as due to cyclotron resonance scattering, the authors estimated a magnetic field of  $\sim 5.3 \times 10^{11}$  G in good agreement with earlier estimates.

In this paper we report on independent discovery of the same feature in *BeppoSAX* observations carried out during the outburst in 1997 (Sect. 3.2)<sup>1</sup> We analyze three *BeppoSAX* observations of GRO J1744–28 carried out during the outburst in 1996–1997 and present a detailed spectral and timing analysis of the persistent flux and the bursts. We also briefly discuss the origin of the bursts in GRO J1744–28. The instruments and methods of the analysis are described in Section 2. Results from the timing and spectral analysis are summarised in Section 3. In Section 4, we discuss the observational results and finally provide a summary of the paper in Section 5.

## 2 OBSERVATIONS

*BeppoSAX* was an Italian X-ray astronomy satellite, with Dutch participation, which operated from 1996 to 2002 (Boella et al. 1997). It covered a broad energy band 0.1–300 keV with four Narrow Field Instruments (NFIs) and two Wide Field Cameras (Jager et al. 1997). The NFIs included the Low-Energy Concentrator Spectrometer (LECS, 0.1–10 keV, Parmar et al. 1997), three identical Medium-Energy Concentrator Spectrometers (MECS, 2–10 keV, Boella et al. 1997), and two collimated high energy detectors with good energy resolution and low instrumental background: the High Pressure Gas Scintillation Proportional Counter (HPGSPC, 4–120 keV, FWHM energy resolution of 8% at 10 keV and 5.5% at 20 keV, Manzo et al. 1997) and the Phoswich Detection System (PDS, 15–300 keV, FWHM energy resolution of 24% at 20 keV, and 14% at 60 keV, Frontera et al. 1997).

GRO J1744–28 was observed by *BeppoSAX* several times from March 1997 to April 1998 (Table 1). In Figure 1 the long term source light curve observed by the All Sky Monitor onboard the Rossi X-ray Timing Explorer (ASM *RXTE*, Bradt et al. 1993) with superimposed *BeppoSAX* observations is presented. The first three observations of *BeppoSAX* were performed in the declining edge of the 1997 outburst, with a total exposure time for MECS of approximately 270 ks. In our work we use LECS, MECS, and PDS in 0.7 – 4 keV, 2 – 10 keV and 15 – 120 keV energy ranges respectively. The HPGSPC was, unfortunately, not operating during the first three observations. In the last three observations, the source was in quiescence and below the sensitivity thresholds of *BeppoSAX*, so it was not detected. The data from the quiescence, however, proved very useful for the background subtraction of the outburst PDS data.

The standard *BeppoSAX* pipeline was used for the processing of the data. HPGSPC and PDS were operated in rocking mode to monitor local background and its variation along the orbit. The

<sup>1</sup> We learned of the content by D’ai et al when the manuscript was in the final steps of preparation.

**Table 1.** Observations of the X-ray source GRO J1744–28 by *BeppoSAX*. Luminosity is estimated using unabsorbed flux in the energy range 2–10 keV (MECS) for the distance  $D = 8$  kpc.

MJD	Exposure time, ks	Period, s	$L_x, 10^{37}$ erg s <sup>-1</sup> 2–10 keV	Orbital phase <sup>a</sup>
50528	117.5	0.467044(1)	2.8	0.9
50534	101.9	0.467044(1)	1.8	0.4
50550	51.6	0.46705(1)	0.46	0.8
50905	62.5	source in		0.8
50911	34.5	quiescent state		0.3
50913	67.5			0.5

<sup>a</sup>Ephemeris from Kouveliotou et al. (1996)

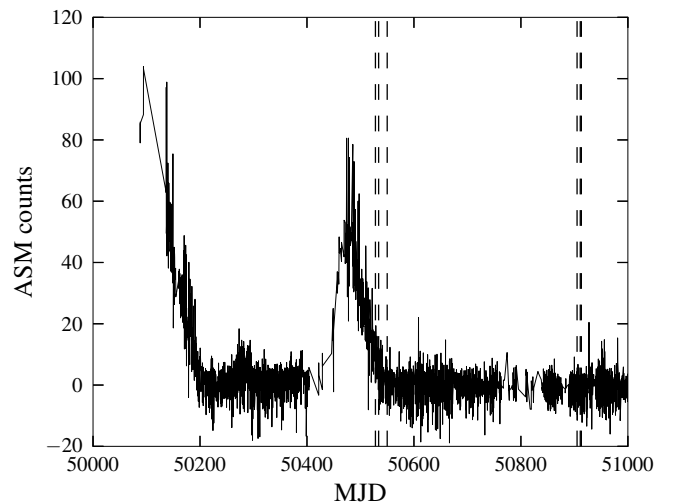


**Figure 1.** The light curve of GRO J1744–28 observed by the ASM onboard *RXTE*. Dashed lines mark the *BeppoSAX* observations (Table 1).

source counts for LECS and MECS were extracted from source centered circles with radii of 4 arcmin, while the background from an annulus with outer radius of 18 arcmin. A detailed description of *BeppoSAX* data reduction procedures can be found in the handbook for *BeppoSAX*.

## 3 DATA ANALYSIS AND RESULTS.

### 3.1 Timing analysis.

The 2–10 keV MECS light curve of the first observation (MJD 50528) is presented in Fig. 2. Bursts are clearly visible in the first two observations, whereas none is detected in the last observation carried out close to the end of the outburst at significantly lower luminosity. We detected 25 and 17 major bursts in the first two observations respectively, with a flux increase of a factor of 10 or more. Typical burst duration and the interval between the bursts are  $\sim 10$  s and  $\sim 2000$  s respectively (see also Fig. 3, where all detected bursts are reported). The inter-burst to burst fluence ratio in the energy range 2–20 keV is between 3 and 18, i.e. compatible with earlier reports (Lewin et al. 1996; Jahoda et al. 1997). The burst profiles exhibit variety of shapes: most are rather symmetric and in this respect are similar to Type II bursts observed in RB (Lewin et al. 1976). However, about twenty percent (for example, the next to last

one in Fig. 3) exhibit the characteristic exponential decay typical of thermonuclear Type I bursts. The source also exhibited a few “smaller” bursts, a factor of  $\sim 6$  less luminous than the major bursts. These have already been reported by Nishiuchi et al. (1999) based on the *ASCA* data. We confirm the presence of the low luminosity bursts, although the statistical quality of the data is not sufficient for any detailed analysis.

As reported earlier by several authors (Lewin et al. 1996; Younes et al. 2015), a flux drop following the burst is a relative common feature in GRO J1744–28. Such a drop is observed in more than half of the bursts in our sample. In Fig. 2 a fragment of the light curve in the 2–10 keV is presented. The decrease of the mean flux from the source after the burst, for about 100 sec, is evident. Note that a similar flux depression is observed after Type II bursts of the RB and is usually associated with the depletion of the inner edge of the accretion disk after the bursting event due to enhanced accretion (Lewin et al. 1996).

To study coherent pulsations, we corrected the photon arrival time for Doppler delays due to the orbital motion of the spacecraft and the pulsar (using the orbital ephemeris of Kouveliotou et al. 1996). Using the phase-connection technique [see for instance] (Doroshenko et al. 2010) we measure the spin period to be  $P = 0.467044(1)$  s,  $P = 0.467050(1)$  s and  $P = 0.46705(1)$  for the March and the two April 1997 observations (all uncertainties are for 90% confidence level unless stated otherwise). Folding the light curves reveals sinusoidal, single-peaked pulse profiles (Fig. 4). We find that the phase of the pulsed profiles during the bursts is shifted by  $\sim 5\%$  relative to the persistent state, which is consistent with earlier reports by Kouveliotou et al. (1996); Strickman et al. (1996). The morphology of the pulse profiles appears to be consistent between the two observations and shows no apparent dependence on luminosity.

The fraction of pulsed emission defined as the ratio  $(F_{\max} - F_{\min}) / (F_{\max} + F_{\min})$ , where  $F_{\max}$  and  $F_{\min}$  are the maximum and minimum source flux does change with energy. To estimate it we assumed standard backgrounds for all instruments and also took the contamination from the nearby sources to the PDS data (see Section 3.2). We found that the pulsed fraction increases between 2 and 10 keV from about 5% to 20% (with a notable exception of a region close to the fluorescent iron line, see also D’Aì et al. 2015), and then remains fairly constant between  $\sim 10\%$  and  $\sim 30\%$  for the first two observations and between 20 – 80% for the third one. From 0.1 to 2 keV, the pulse fraction decreases from 20 – 30% to 5% although our findings are at the lowest energies and for the third observation are hampered by low statistics (Fig. 5).

### 3.2 Spectral analysis.

GRO J1744–28 is located in the crowded Galactic Center region and a number of sources fall into the field of view of the telescope. This might potentially affect the spectral analysis, particularly for non-imaging instruments. Even the LECS and MECS observations could be affected as the deep *Chandra* observation of the field reveals  $\sim 40$  sources within the standard  $4'$  extraction region. However, GRO J1744–28 is by far the brightest among these sources even in quiescence, so for the imaging instruments MECS and LECS source confusion is not an issue. We followed, therefore, standard analysis procedure.

The situation for the non-imaging instruments is more complicated. The MECS image reveals at least two sources besides GRO J1744–28 within the field of view of collimating instruments. These are detected irrespective of the brightness of the pul-

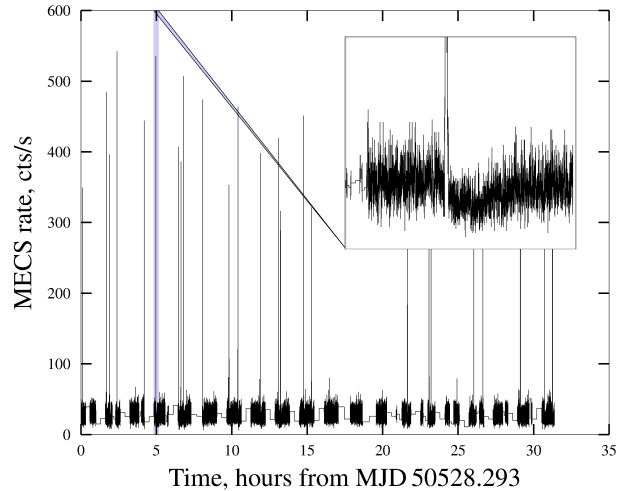


**Figure 2.** MECS light curve with bursts of the pulsar GRO J1744–28 in 1997-03-21 with 2 s bin time in 2 – 10 keV energy range. On the zoom picture the flux drop after the burst is shown.

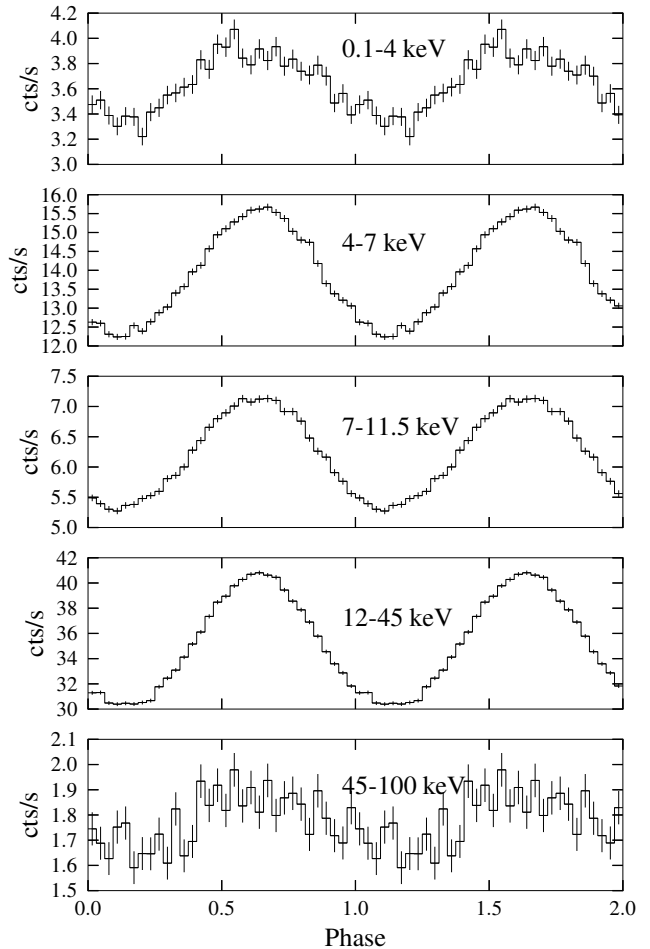


**Figure 4.** Pulse profiles of the pulsar GRO J1744–28 in 1997-03-21 for LECS (0.1 – 4 keV), MECS (4 – 7 – 11.5 keV) and PDS (12 – 45 – 100 keV). The spin period is  $P = 0.467044(1)$  s.

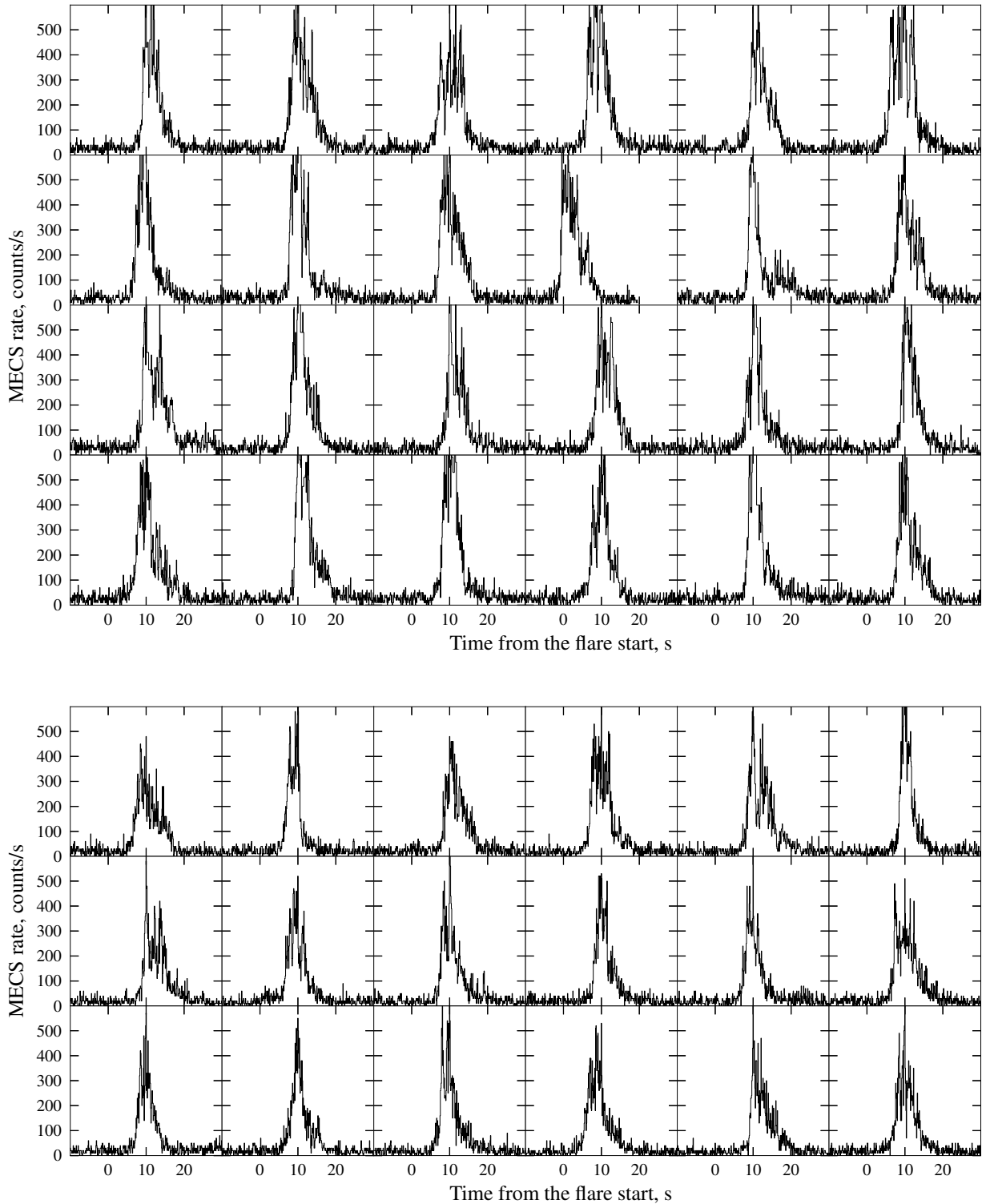


**Figure 3.** Light curves of all burst of the pulsar GRO J1744–28 in 1997-03-21 (top) and 1997-03-27 (bottom), MECS.

sar (see Fig. 6) and are plausibly identified as 1E 1743.1-2843 and Sgr A\*. To account for the in-orbit instrumental background which is rapidly changing and the for the contribution of the sources contaminating the PDS data, we extracted the background-subtracted spectra for all observations (including those in quiescence) using

the standard pipeline. The standard pipeline allows to account for instrumental in-orbit background. Then we subtracted quiescent spectra (obtained during the 1998 observations) from the source spectra obtained for the first three observations. Apparently, an important assumption here is that the flux of the contaminating

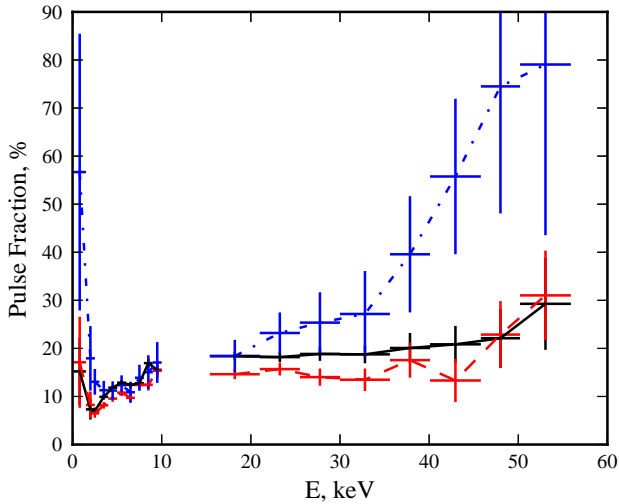


**Figure 5.** Pulse fraction of the pulsar GRO J1744–28 for 1997-03-21 - solid black line, 1997-03-27 - dashed red line, 1997-04-12 - dashed dotted blue line.

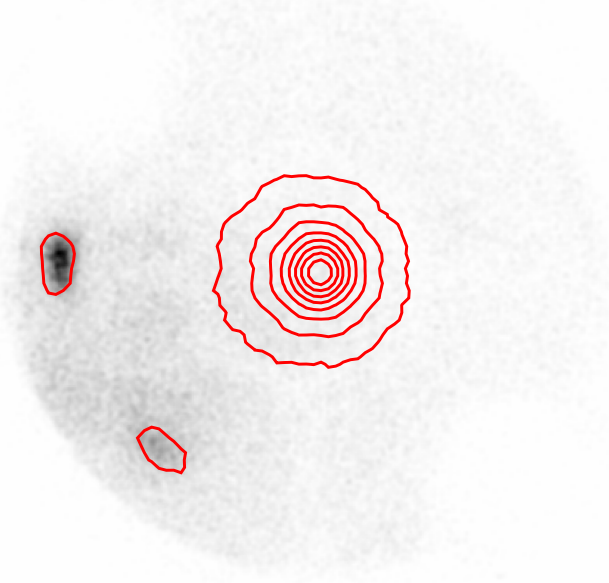


**Figure 6.** MECS image centered at GRO J1744–28 in quiescence on 1998-04-02 overlaid with contours from an observation in bright state (taken on 1997-03-21). Two additional sources detected in the MECS field of view contaminate also the PDS spectrum.

sources remains constant. To verify that we compared the soft X-ray fluxes measured by the MECS which indeed remained constant.

For spectral fitting, we used the XSPEC package (version 11.3.2, Arnaud 1996). We found that the observed broadband continuum spectrum can be described with several phenomenological models generally used for the spectra of accreting X-ray pulsars:

1) a power law plus a high-energy cutoff model, where the transition is smoothed with a Gaussian

$$PHC \sim E^{-\Gamma} \begin{cases} 1 & (E \leq E_{cut}) \\ e^{-(E-E_{cut})/E_{fold}} & (E > E_{cut}) \end{cases};$$

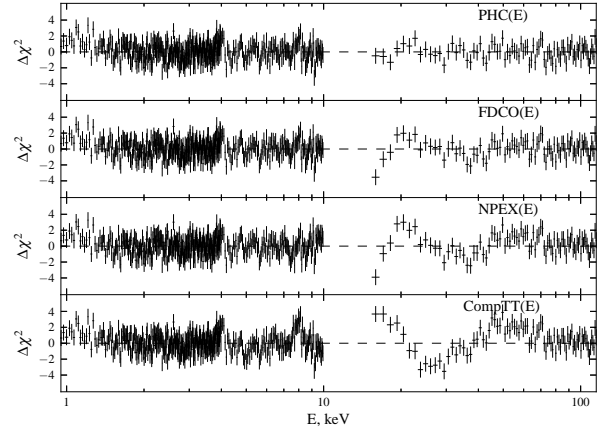


**Figure 7.** The best-fit residuals for spectra derived from the observation 1997-03-21 modeled as described in the main text. The best residuals obtained with the power law plus high-energy cutoff model, *PHC*(*E*), at the top panel.

2) a power law with Fermi-Dirac cutoff:

$$FDCO \sim E^{-\Gamma} (1 + e^{(E-E_{cut})/E_{fold}})^{-1};$$

3) the Negative and Positive power law EXponential model (Mihara 1995; Makishima et al. 1999):

$$NPEX = (A_1 E^{-\alpha_1} + A_2 E^{+\alpha_2}) e^{-E/E_{fold}};$$

4) the *CompTT* model by Titarchuk (1994) describing the comptonization of soft photons with temperature  $kT_s$  in a hot electron plasma with  $kT_e$  and a hot electron optical depth  $\tau_e$ .

In all cases the inclusion of the fluorescent iron  $K_{\alpha}$  line at  $\sim 6.7$  keV (modelled with a simple Gaussian profile) was also required. All continuum models give a reasonably good  $\chi^2_{red}$  (from 0.94 for the *PHC* model to 1.25 for *CompTT* model, see Table 2). To demonstrate the evolution of the parameters with the luminosity we used *PHC* based on the formal statistical quality and stability of the fit (Table 3). Regardless of the assumed continuum model, some residuals below 1 keV, and around 4–5 keV (Fig. 8) were clearly observed. The absorption-like feature at  $\sim 4$  keV was modelled with a multiplicative line with either a gaussian or lorentzian profile. This significantly improved the fit (see residuals of Fig. 8). The parameters of the line for the gaussian profile are presented in Table 2. For the lorentzian profile (CYCLABS in XSPEC) we get comparable values, i.e.  $E_{cyc} = 4.0 \pm 0.2$  keV,  $\sigma = 1.3 \pm 0.2$  keV. The chance probability for fit improvement based on the f-test is marginal  $\leq 10^{-30}$  (see, however, Protassov et al. 2002). The feature also appeared in the phase resolved spectra (see Fig. 9). Our findings nicely agrees with the absorption-like feature recently reported by D’Ai et al. (2015) based on *XMM-Newton* and *INTEGRAL* observations of the 2014 outburst. We note that Younes et al. (2015) detected an absorption feature at 10 keV which is not observed in our data, although the lack of HPGSPC data makes it difficult to draw a definitive conclusion.

We have also performed a pulse phase resolved spectral analysis to study the variation of spectral parameters with the angle of view to the neutron star. Only data from the observation on March 21, 1997 with highest luminosity and best counting statistics was considered. To describe the phase resolved spectra, we used the same model as for the phase averaged spectrum, i. e. a power law



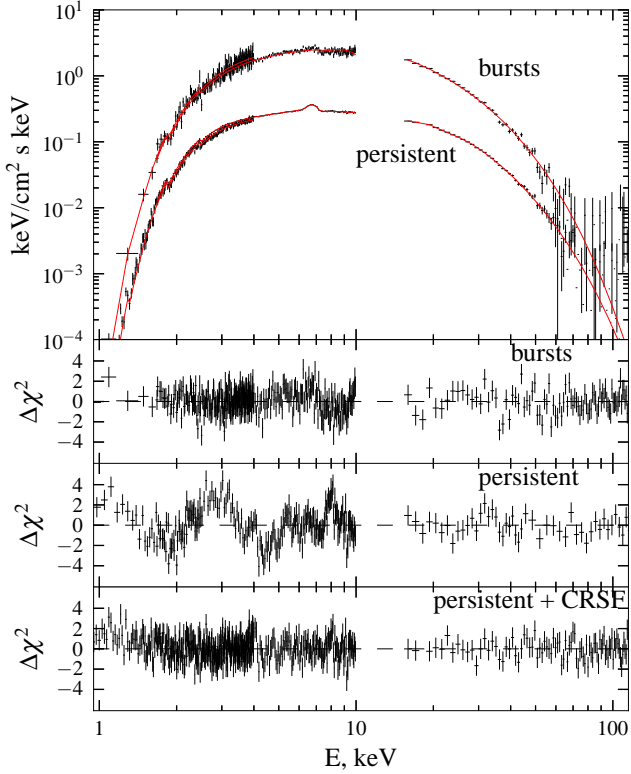


**Figure 8.** The best-fit unfolded average persistent spectrum, modelled with the *PHC* continuum is shown in the top panel. We also present the best fit residuals without and with the inclusion of a cyclotron line at  $\sim 4.5$  keV. The best fit spectrum of the bursts modelled with *PHC* and a black body continuum is also presented together with the residuals for the observation 1997-03-21.

**Table 2.** Spectral parameters of the persistent spectrum of GRO J1744–28 observed by *BeppoSAX* in 1997-03-21 for various spectral models. All energies and line widths are given in keV.

Par.	<i>PHC</i>	<i>PHC</i> no CRSE	<i>FDCO</i>	<i>NPEX</i>	<i>CompTT</i>
$N_{\text{H}}^{\text{a}}$	5.7(2)	5.23(2)	5.55(8)	5.16(6)	5.84(3)
$\Gamma$	1.26(7)	1.147(3)	1.09(4)		
$E_{\text{cut}}$	18.4(1)	18.1(1)	15(1)		
$E_{\text{fold}}$	11.7(4)	11.76(7)	10.2(2)	6.1(1)	
$\alpha_1$				0.48(4)	
$\alpha_2$				-2.0	
$kT_{\text{s}}$					0.18(3)
$kT_{\text{e}}$					5.82(3)
$\tau_{\text{e}}$					13.1(1)
$E_{\text{Fe}}$	6.69(2)	6.71(2)	6.70(2)	6.68(2)	6.72(2)
$\sigma_{\text{Fe}}$	0.28(3)	0.38(2)	0.26(3)	0.23(3)	0.34(3)
$N_{\text{Fe}}^{\text{b}}$	7.2(6)	10.2(4)	5.8(5)	5.8(6)	8.8(5)
$E_{\text{cyc}}$	4.3(2)		4.47(9)	4.55(5)	4.2(3)
$\sigma_{\text{cyc}}$	1.2(3)		1.1(2)	1.2(1)	0.7(5)
$\chi^2_{\text{red}}/\text{dof}$	0.94 / 549	1.28 / 552	0.95 / 551	1.04 / 551	1.25 / 553

<sup>a</sup>in units  $10^{22}$  atoms  $\text{cm}^{-2}$

<sup>b</sup> $K_{\alpha}$  line normalization in units  $10^{-3}$  ph  $\text{cm}^{-2}$   $\text{s}^{-1}$

**Table 3.** Spectral parameters of the persistent spectrum low mass X-ray pulsar GRO J1744–28 observed by *BeppoSAX* modeling by the *PHC* with smoothing gaussian continuum model. All the energies and the line widths are given in keV.

Parameter	1997-03-21	1997-03-27	1997-04-12
$N_{\text{H}}^{\text{a}}$	5.7(2)	5.7(2)	5.4(1)
$\Gamma$	1.26(7)	1.29(5)	1.24(3)
$E_{\text{cut}}$	18(1)	19.3(8)	24(4)
$E_{\text{fold}}$	11.7(4)	13.3(5)	12(3)
$E_{\text{Fe}}$	6.69(2)	6.70(3)	6.68(5)
$\sigma_{\text{Fe}}$	0.28(3)	0.27(4)	0.24(7)
$N_{\text{Fe}}^{\text{b}}$	7.2(7)	4.9(6)	1.2(2)
$E_{\text{cyc}}$	4.3(2)	4.3(1)	
$\sigma_{\text{cyc}}$	1.2(3)	1.1(1)	
$F_{\text{Fe}}^{\text{c}}$	10.1	6.5	1.2
$F_{\text{unab}}^{\text{c}}$	13.0	8.3	1.6
$\chi^2_{\text{red}}/\text{dof}$	0.94 / 549	1.04 / 531	1.06 / 487

<sup>a</sup>in units  $10^{22}$  atoms  $\text{cm}^{-2}$

<sup>b</sup> $K_{\alpha}$  line normalization in units  $10^{-3}$  ph  $\text{cm}^{-2}$   $\text{s}^{-1}$

<sup>c</sup>Absorbed and unabsorbed fluxes in units  $10^{-9}$  erg  $\text{cm}^{-2}$   $\text{s}^{-1}$  and in 0.1 – 120 keV range.

with high-energy cut-off (see Fig. 9). We divided the data in 10 equally spaced phase bins. We fixed the absorption component at the average value  $N_{\text{H}} = 5.7^{+0.2}_{-0.2} \times 10^{22}$  atoms  $\text{cm}^{-2}$ . The emission iron line at  $\sim 6.7$  keV and the absorption-like feature at  $\sim 4.5$  keV were also included in the phase resolved analysis. We can see the clear anti-correlation of the photon index with phase flux. The parameters of the absorption-like and iron lines (line centroid and width) did not exhibit any significant phase variation. The cut-off and folding energies appeared to be anti-correlated with each other.

### 3.2.1 Analysis of the burst spectra

To investigate the burst spectra we aligned and stacked all observed bursts using the rising edge as a reference to improve statistics. We also subtracted the contribution of the persistent emission. We found that the shape of the combined spectrum of the bursts departs significantly from that of the non-bursting spectrum (Fig.8).

We first described the burst spectrum with the *PHC* and *CompTT* models. Both models give formally acceptable results (see Table 4). The spectral parameters of the *PHC* model are similar to the ones reported recently by Younes et al. (2015) for the burst spectra ( $\Gamma = 0.2 \pm 0.1$  and  $E_{\text{fold}} = 7.6 \pm 0.5$  keV). Such a hard power law together with a soft cut-off are rather peculiar and not typical of X-ray pulsars. This might suggest that the model describes a bump-like feature at soft energies. In addition, the best-fit results for the bursts spectrum using the *CompTT* model reveals a significant change, with respect to the persistent spectrum, of both the seed photon temperature and the absorption column (see Table 4), which is difficult to understand. On the other hand, the apparent change of the seed photon temperature might suggest an additional soft component in the burst spectrum. Indeed, including a blackbody component in either model allows to achieve comparable (or, in fact, slightly better) fit statistics while the other parameters of the continuum remain close to ones measured for the persistent spectrum. In other words, we find that the burst spectrum significantly differs from the persistent one at soft energies, and this change is well accounted for by adding a soft blackbody-like component to

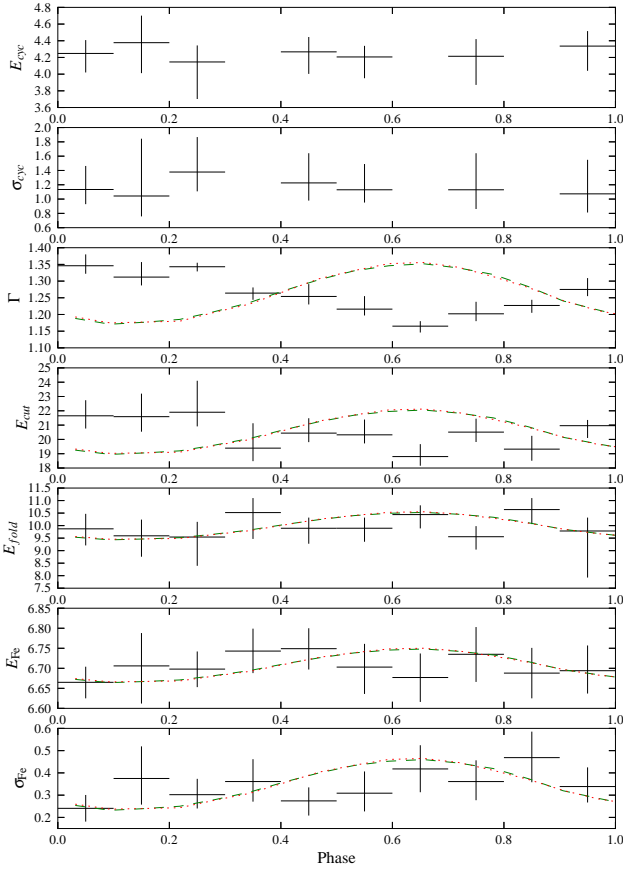


**Figure 9.** Spectral parameters of the pulsar GRO J1744–28 in 1997-03-21 with the *PHC* continuum model as function of pulse phase. Phase: 0-0.2-0.4-0.6-0.8-1. Dashed lines are the MECS and PDS pulse profiles, they are the same.

the unchanged continuum of the persistent spectrum. The black-body component has a temperature about 2.1 – 2.2 keV and a size close to a neutron star radius (for an assumed distance of 8 kpc). A Fe-K line is also marginally significant in the burst spectra of the observation on 1997-03-27. We have summarised the fit results for the 1997-03-21 data in Table 4.

To investigate the pulse phase dependence of the black body and power law components we carried out the phase resolved analysis of the burst spectrum. Unfortunately, the statistics was insufficient to constrain all model parameters, so we kept most of the parameters fixed to the best-fit phase average values, and only allowed the normalizations of the continuum components to vary. The results are shown in Fig. 10. The pulse fraction for the soft and hard components are  $6.5\% \pm 3.4\%$  and  $13.8\% \pm 1.9\%$  respectively, i.e. the hard component varies with pulse-phase stronger than the soft one.

To explore the time evolution of both components along the burst, we performed also time-resolved spectral analysis using the stacked data of all bursts. It is interesting to note, that both the temperature and normalization of the blackbody component (and thus the size of the emitting region) change along the burst as shown in Figure 11.

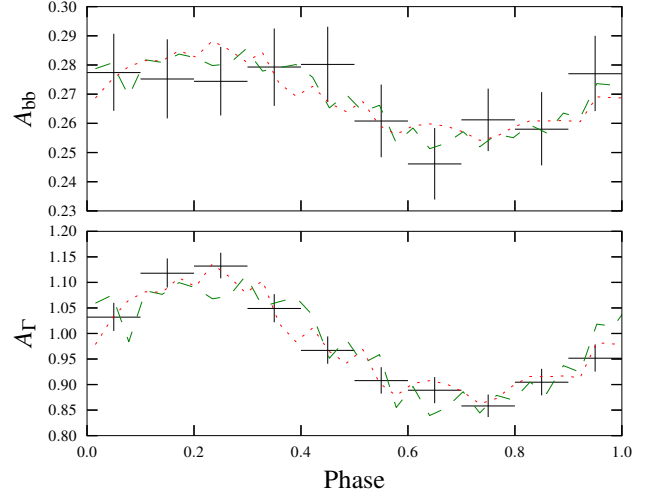


**Figure 10.** Changing normalizations of the soft (top) and hard (bottom) part of the bursts spectrum with phase for the GRO J1744–28 in 1997-09-21.  $\chi^2_{\text{red}}$  lies in region from 0.97 to 1.45.

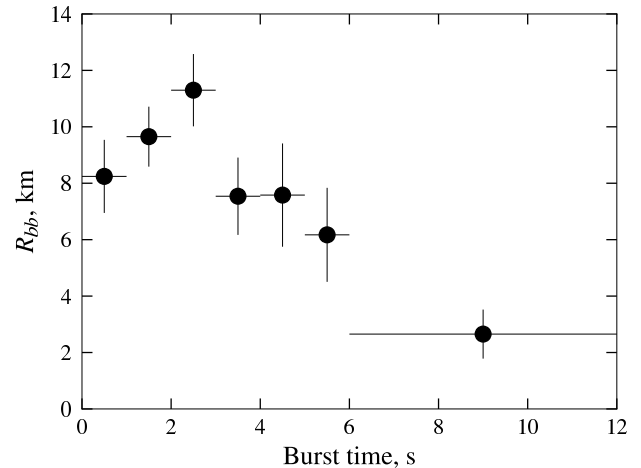
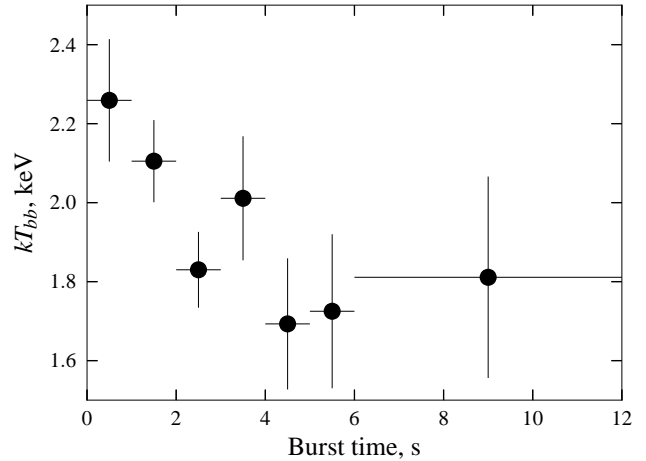


**Figure 11.** Cooling of the soft component, during the bursts. The probability that the observed temperatures are due to a statistical fluctuation is  $\leq 1.7 \times 10^{-8}$  (from Kolmogorov-Smirnov test), so the trend is significant.

**Table 4.** Best-fit parameters of the bursts spectrum GRO J1744–28 in 1997-201. All the energies and the line widths are given in keV.

Parameter	<i>PHC</i>	<i>bb+PHC</i>	<i>CompTT</i>	<i>bb+CompTT</i>
$N_{\text{H}}^a$	5.0(3)	5.1(7)	3.4(2)	5.2
$kT_{\text{bb}}$		2.1(3)		2.2(1)
$R_{\text{bb}}^b$		$\sim 7.5$		$\sim 7.6$
$\Gamma$	0.26(8)	0.8(4)		
$E_{\text{cut}}$	4(1)	18(5)		
$E_{\text{fold}}$	7.6(2)	9(1)		
$kT_{\text{s}}$			1.51(8)	0.2
$kT_{\text{e}}$			5.4(2)	5.2(1)
$\tau_{\text{e}}$			4.6(5)	18(1)
$\chi^2_{\text{red}}/\text{dof}$	0.96 / 408	0.95 / 406	1.03 / 409	1.02 / 409

<sup>a</sup>in units  $10^{22}$  atoms  $\text{cm}^{-2}$ , <sup>b</sup>in km. The absorbed and unabsorbed fluxes in 0.1 – 120 keV energy range are  $F_{\text{ab}} = 6.09 \times 10^{-8}$  erg  $\text{cm}^{-2}$   $\text{s}^{-1}$ ,  $F_{\text{unab}} = 6.83 \times 10^{-8}$  erg  $\text{cm}^{-2}$   $\text{s}^{-1}$ .

#### 4 DISCUSSION

The non-bursting spectrum of GRO J1744–28 has been measured for the first time in a broad energy range 0.7 to 120 keV with *BepoSAX* during the source outburst in 1996-1997. The persistent spectrum of the source is similar to the one of accreting pulsars and can be described by phenomenological models typically used for pulsars, e.g. by an absorbed power law with cut-off at around  $\sim 18$  keV. In addition, a line-like absorption feature at  $E \sim 4.5$  keV is observed and required regardless of the used continuum model. We incidentally observe that there are no systematic effects known for the MECS and LECS, in the energy range where residuals are observed. In addition, this absorption-like feature is not observed in the spectrum of the bursts, which has similar shape and comparable statistical quality. Therefore, the feature is unlikely to be an artefact of the continuum modelling.

Cyclotron resonance scattering features (CRSFs), interpreted as a result of resonant scattering of continuum photons off plasma electrons in strong magnetic fields close to the electron gyro frequency, are often observed in the spectra of accreting pulsars. CRSFs appears as a flux suppression of the continuum at cyclotron energies related to the magnetic field strength in the line forming region:

$$E_{\text{cyc}} \approx 11.57 B_{12} (1+z)^{-1} \text{ keV},$$

where  $B_{12}$  is the magnetic field strength in the units of  $10^{12}$  G,  $z$  is the gravitational redshift (see Pottschmidt et al. (2012), Doroshenko et al. (2010), Santangelo et al. (1999) for a recent review). By interpreting an absorption-like feature observed at  $E \sim 4.5$  keV in the spectrum of GRO J1744–28 as a CRSF, a magnetic field of  $B \sim 3.7 \times 10^{11} (1+z)$  G is obtained for the neutron star of the binary system. This is in strikingly good agreement with earlier estimates of the magnetic field of this pulsar, which fall in range  $2.7 \times 10^{11}$  G (Finger et al. 1996; Rappaport & Joss 1997; Cui 1997) and (Younes et al. 2015; D’Ai et al. 2015).

In particular, D’Ai et al. (2015) have recently reported the detection of such an absorption feature at  $\sim 4.7$  keV based on *XMM-Newton* and *INTEGRAL* data, which they also interpret as a cyclotron resonance scattering feature (CRSF). Our result is in excellent agreement with these findings.

Besides the lack absence of absorption feature, the burst spectrum was found to differ significantly from the non-bursting spec-

trum, particularly at soft energies. The difference is most easily accounted for by inclusion of a black-body component on top of the power law-like persistent spectrum of accreting pulsars. The flux in 0.7 – 120 keV energy range measured for the power law and the blackbody components is  $F_{\text{bb}} \approx 1.6 \times 10^{-8}$  erg  $\text{cm}^{-2}$   $\text{s}^{-1}$  and  $F_{\text{power}} \approx 4 \times 10^{-8}$  erg  $\text{cm}^{-2}$   $\text{s}^{-1}$ , respectively. This indicates that  $\sim 30\%$  of the energy released in bursts arises from the soft thermal component not present in the persistent emission.

The nature of the soft component is unclear and several hypotheses may be considered. First of all, spectra of accreting pulsars are known to change with luminosity and the luminosity in GRO J1744–28 increases by an order of magnitude during the bursts, so some intrinsic variation of the spectrum might be anticipated. For instance, Reig & Nespoli (2013) reported evident spectral softening for several pulsars above the so-called critical luminosity  $\sim 10^{37}$  erg  $\text{s}^{-1}$  (Basko & Sunyaev 1976; Mushtukov et al. 2015), and similar softening might occur in GRO J1744–28, which at  $L_x \sim 10^{38}$  erg  $\text{s}^{-1}$  is likely also above this limit.

Emission from the accretion column expected to form at this stage can also irradiate the accretion disk or the surface of neutron star (Lyubarskii & Syunyaev 1988; Poutanen et al. 2013), and the thermalization of intercepted emission could be responsible for the soft component as well. The effective temperature of the irradiated surface  $T_{\text{eff}} \approx (L_x/4\pi r^2/\sigma_{\text{SB}})^{1/4} \sim 2$  keV is, in fact, comparable with the observed. On the other hand, strong gravitational separation of chemical elements in the neutron star atmospheres (Hameury et al. 1983) implies that the upper atmospheric layers consist almost exclusively of fully ionized hydrogen plasma which reflects most of the incident flux due to electron scattering. Therefore, the fraction of thermalized emission is likely to be less than 10% (see a detail argumentation in Poutanen et al. 2013), in contrast with the  $\sim 30\%$  observed. It is also hard to explain the observed pulsation of the soft component if it originates in the inner regions of accretion disk, although the even softer component with  $kT \sim 0.5$  keV reported recently by Younes et al. (2015); D’Ai et al. (2015) might indeed be related to irradiation of the accretion disk by the pulsar.

Finally, taking into consideration the observed cooling of the thermal component along the burst (see Fig. 11) very similar to that observed in classical bursters (Lewin et al. 1993) thermonuclear flashes on the NS surface could be also responsible for the observed soft emission. In fact, several authors have already considered the possibility that some of the bursts in GRO J1744–28 might be Type-I bursts. Based on the *BATSE* observations, Lewin et al. (1996) concluded that this is unlikely because the amount of matter accreted between the bursts is insufficient to explain the observed burst fluence if bursts are powered by thermonuclear burning. Indeed, the inter-burst to burst fluence ratio  $\alpha \sim 4$  deduced from *BATSE* observations was found to be much smaller than  $\alpha \geq 40$  typical of thermonuclear hydrogen burning (Lewin et al. 1993).

On the other hand, Jahoda et al. (1997), based on the *RXTE* observations close to the peak of the outburst, found significantly higher  $\alpha \sim 34$ . Moreover, we found that the flux of the thermal component constitutes only about 30% of the total flux and, and therefore of the burst fluence. If this is taken into account, even at lower luminosities such as during the *BeppoSAX* observations, when we estimate  $\alpha \sim 5 - 15$  for the bolometric flux, the same ratio calculated for the thermal component alone is factor of three higher, i.e. still comparable with that observed in classical bursters. Therefore the argument by Lewin et al. (1996) clearly does not always hold.

The strongest argument against the thermonuclear origin of



the soft component in burst spectrum of GRO J1744–28 is that it is an accreting pulsar. Indeed, the temperature and pressure of matter funneled by the magnetic field to the polar areas are usually sufficient for stable thermonuclear burning, so no unburned matter accumulates at the surface and thus no Type-I bursts are observed from accreting pulsars. In fact, Bildsten & Brown (1997) did consider the possibility of unstable thermonuclear burning in GRO J1744–28, and concluded that under the most favourable assumptions it should not be possible. In particular, Bildsten & Brown (1997) argue that to escape the accretion flow and spread over the NS surface (where it can be accumulated and subsequently ignite as a thermonuclear flash), the accreted plasma must overcome the magnetic pressure and turn the magnetic field lines parallel to the neutron star surface. This implies a pressure of  $P \approx 10^{24} \text{ erg cm}^{-3}$  while the hydrogen/helium mixture burns in the stable regime at  $P \approx 10^{22} \text{ erg cm}^{-3}$ .

In other words, accreting matter remains confined at the polar caps where it burns steadily as expected. However, in our opinion, this key assumption of Bildsten & Brown (1997) is probably too conservative, and, in fact, corresponds to the case when the plasma is not confined to polar areas at all. This would basically imply that GRO J1744–28 is an ordinary burster, which clearly it is not. On the other hand, the magnetic pressure at the poles of the neutron star can be estimated based on the observed CRSF energy and turns out to be  $B^2/8\pi \approx 10^{22} \text{ erg cm}^{-3}$  comparable with the pressure required for stable thermonuclear burning. Therefore, the magnetic field is unlikely to confine plasma at significantly higher pressures and part of accreted matter probably leaves the polar areas before burning, thereby creating conditions for thermonuclear flashes. We note also that, if realised, the onset of a such flash could in principle disrupt the inner parts of the accretion disk triggering the instabilities responsible for the enhanced accretion rate and most of the observed burst emission.

In conclusion, we fully agree that there is no doubt that the mass accretion rate does increase during the bursts GRO J1744–28 and is responsible for the bulk of the observed emission. However, some fraction of the flux in principle could still be due to unstable thermonuclear burning at the NS surface.

## 5 SUMMARY AND CONCLUSIONS

We presented the results of the analysis of three *BeppoSAX* observations, with a total exposure time 270 ks, carried out in the declining phase of the 1997 outburst of the unique bursting pulsar GRO J1744–28.

Pulsations with a period of 0.4670 s with a stable pulse profile were detected in all observations. The pulsed fraction was found to vary with energy, reaching a minimum of 10–20% in the energy range 5–40 keV and increasing for higher and lower energies, especially at lower luminosities. Several tens of bursts with typical durations of about 10 s were detected as well. Depletion in the light curve is observed after at least some of the bursts. The source luminosity typically increases by factor of ten during the bursts, although a number of dimmer bursts are also observed.

The non-bursting broad band X-ray spectrum was found to be well described by several phenomenological models typically used for accreting pulsars. An iron line at  $\sim 6.7$  keV and an absorption feature at  $\sim 4.5$  keV were also required to fit the data. We interpret the absorption feature as a cyclotron line which implies a magnetic field of the neutron star of  $B \sim 3.7 \times 10^{11}$  G. This value is in good agreement with earlier predictions and with the recent ob-

servations of the 2014 outburst with *XMM-Newton* and *INTEGRAL*. D’Ai et al. (2015) have detected the same feature at  $E \sim 4.7$  keV in agreement, within uncertainties, with our measurement.

The average burst spectrum could be represented as a combination of the harder non-bursting spectrum and an additional soft thermal component with temperature of about 2 keV. The burst spectrum requires that neither the iron 6.7 keV line nor the absorption feature at 4.5 keV. Both components are pulsed although the amplitude is smaller for the soft component,  $\sim 6.5\%$  vs  $\sim 13.8\%$ .

We discussed a possible nature of the thermal component and speculate that it could be caused by thermonuclear flashes which possibly trigger the accretion rate enhancement responsible for the bursts observed in the source. This hypothesis is based on several similarities between typical Type I bursts and the thermal component, namely, the burst duration of 10 s, the inter-burst to burst fluence ratio and cooling as a burst progresses. There are some observational and theoretical arguments that disfavor this hypothesis. These cannot be verified with the existing data, however, additional data from current or future missions like LOFT (in ’t Zand et al. 2015) might provide decisive insights on this puzzling source.

## ACKNOWLEDGEMENTS

This work is partially supported by the Bundesministerium für Wirtschaft und Technologie through the Deutsches Zentrum für Luft und Raumfahrt (DLR, Grants FKZ 50 OG 1001, 50 OR 0702, 50 QR 1008), the German Research Foundation (DFG) grant WE 1312/48-1.

## REFERENCES

- Arnaud K. A., 1996, *Astronomical Data Analysis Software and Systems V*, 101, 17
- Basko M. M., Sunyaev R. A., 1976, *MNRAS*, 175, 395
- Bildsten L., Brown E. F., 1997, *ApJ*, 477, 897
- Boella G., Butler R. C., Perola G. C., Piro L., Scarsi L., Bleeker J. A. M., 1997, *A&AS*, 122, 299
- Boella G., Chiappetti L., Conti G., Cusumano G., del Sordo S., Rosa G. L., Maccarone M. C., Mineo T., Molendi S., Re S., Sacco B., Tripiciano M., 1997, *A&AS*, 122, 327
- Bradt H. V., Rothschild R. E., Swank J. H., 1993, *A&AS*, 97, 355
- Cui W., 1997, *ApJ*, 482, L163
- D’Ai A., Di Salvo T., Iaria R., García J. A., Sanna A., Pintore F., Riggio A., Burderi L., Bozzo E., Dauser T., Matranga M., Galiano C. G., Robba N. R., 2015, *MNRAS*
- Daigne F., Gondoni P., Ferrando P., Goldwurm A., Decourchelle A., Warwick R. S., 2002, *A&A*, 386, 531
- Daumerie P., Kalogera V., Lamb F. K., Psaltis D., 1996, *Nature*, 382, 141
- Degenaar N., Miller J. M., Harrison F. A., Kennea J. A., Kouveliotou C., Younes G., 2014, *ApJ*, 796, L9
- Degenaar N., Wijnands R., Cackett E. M., Homan J., in ’t Zand J. J. M., Kuulkers E., Maccarone T. J., van der Klis M., 2012, *A&A*, 545, A49
- Doroshenko V., Santangelo A., Suleimanov V., Kreykenbohm I., Staubert R., Ferrigno C., Klochkov D., 2010, *A&A*, 515, 10
- Dotani T., Ueda Y., Ishida M., Nagase F., Inoue H., Saitoh Y., 1996, *IAU Circ.*, 6337, 1
- Finger M. H., Koh D. T., Nelson R. W., Prince T. A., Vaughan B. A., Wilson R. B., 1996, *Nature*, 381, 291

- Fishman G. J., Kouveliotou C., van Paradijs J., Harmon B. A., Pacieras W. S., Briggs M. S., Kommers J., Lewin W. H. G., 1995, *IAU Circ.*, 6272, 1
- Frontera F., Costa E., dal Fiume D., Feroci M., Nicastro L., Orlandini M., Palazzi E., Zavattini G., 1997, *A&AS*, 122, 357
- Hameury J. M., Heyvaerts J., Bonazzola S., 1983, *A&A*, 121, 259
- Illarionov A. F., Sunyaev R. A., 1975, *A&A*, 39, 185
- in 't Zand J. J. M., Altamirano D., Ballantyne D. R., Bhattacharyya S., Brown E. F., Cavecchi Y., Chakrabarty D., Chenvez J., Cumming A., Degenaar N., Falanga M., Galloway 2015, *ArXiv e-prints*
- Jager R., Mels W. A., Brinkman A. C., Galama M. Y., Goulooze H., Heise J., Lowes P., Muller J. M., Naber A., Rook A., Schuurhof R., Schuurmans J. J., Wiersma G., 1997, *A&AS*, 125, 557
- Jahoda K., Stark M. J., Strohmayer T. E., Zhang W., Morgan E. H., Fox D., 1997, *ArXiv Astrophysics e-prints*
- Kouveliotou C., van Paradijs J., Fishman G. J., Briggs M. S., Kommers J., Harmon B. A., Meegan C. A., Lewin W. H. G., 1996, *Nature*, 379, 799
- Lewin W. H. G., Doty J., Clark G. W., Rappaport S. A., Bradt H. V. D., Doxsey R., Hearn D. R., Hoffman J. A., Jernigan J. G., Li F. K., Mayer W., McClintock J., Primini F., Richardson J., 1976, *ApJ*, 207, L95
- Lewin W. H. G., Rutledge R. E., Kommers J. M., van Paradijs J., Kouveliotou C., 1996, *ApJ*, 462, L39
- Lewin W. H. G., van Paradijs J., Taam R. E., 1993, *Space Sci. Rev.*, 62, 223
- Lyubarskii Y. E., Syunyaev R. A., 1988, *Soviet Astronomy Letters*, 14, 390
- Makishima K., Mihara T., Nagase F., Tanaka Y., 1999, *ApJ*, 525, 978
- Manzo G., Giarrusso S., Santangelo A., Ciralli F., Fazio G., Piraino S., Segreto A., 1997, *A&AS*, 122, 341
- Mihara T., 1995, Ph.D. thesis, p. 215
- Miller G. S., 1996, *ApJ*, 468, L29
- Mushtukov A. A., Suleimanov V. F., Tsygankov S. S., Poutanen J., 2015, *MNRAS*, 447, 1847
- Nishiuchi M., Koyama K., Maeda Y., Asai K., Dotani T., Inoue H., Mitsuda K., Nagase F., Ueda Y., Kouveliotou C., 1999, *ApJ*, 517, 436
- Parmar A. N., Martin D. D. E., Bavdaz M., Favata F., Kuulkers E., Vacanti G., Lammers U., Peacock A., Taylor B. G., 1997, *A&AS*, 122, 309
- Pottschmidt K., Suchy S., Rivers E., Rothschild R. E., Marcu D. M., Barragán L., Kühnel M., 2012, in Petre R., Mitsuda K., Angelini L., eds, *American Institute of Physics Conference Series Vol. 1427*. pp 60–67
- Poutanen J., Mushtukov A. A., Suleimanov V. F., Tsygankov S. S., Nagirner D. I., Doroshenko V., Lutovinov A. A., 2013, *ApJ*, 777, 115
- Protassov R., van Dyk D. A., Connors A., Kashyap V. L., Siemiginowska A., 2002, *ApJ*, 571, 545
- Rappaport S., Joss P. C., 1997, *ApJ*, 486, 435
- Reig P., Nespoli E., 2013, *A&A*, 551, A1
- Santangelo A., Segreto A., Giarrusso S., dal Fiume D., Orlandini M., Parmar A. N., Oosterbroek T., Bulik T., Mihara T., Campana S., Israel G. L., Stella L., 1999, *ApJ*, 523, L85
- Strickman M. S., Dermer C. D., Grove J. E., Johnson W. N., Jung G. V., Kurfess J. D., Philips B. F., Share G. H., Sturner S. J., Messina D. C., Matz S. M., 1996, *ApJ*, 464, L131
- Sturner S. J., Dermer C. D., 1996, *ApJ*, 465, L31
- Titarchuk L., 1994, *ApJ*, 434, 570
- Wijnands R., Wang Q. D., 2002, *ApJ*, 568, L93
- Woods P. M., Kouveliotou C., van Paradijs J., Briggs M. S., Wilson C. A., Deal K., Harmon B. A., Fishman G. J., Lewin W. H. G., Kommers J., 1999, *ApJ*, 517, 431
- Younes G., Kouveliotou C., Grefenstette B. W., Tomsick J. A., Tennant A., Finger M. H., Furst F., Pottschmidt K., Bhalerao V., Boggs S. E., Boirin L., Chakrabarty D., Christensen F. E., Craig W. W., Degenaar N., Fabian A. C., 2015, *ApJ*